THE PUBLISHING HOUSE
OF THE ROMANIAN ACADEMY

PROCEEDINGS OF THE ROMANIAN ACADEMY, Series A,
Volume 20, Number 1/2019, pp. 97–104

INFORMATION SCIENCE

RETINAL VESSEL LABELLING METHOD

Florin ROTARU, Silviu-Ioan BEJINARIU

Institute of Computer Science, Romanian Academy Iasi Branch
Str. T. Codrescu nr.2, 700481, Iaşi, Romania
Corresponding author: Silviu-Ioan BEJINARIU, E-mail: silviu.bejinariu@iit.academiaromana-is.ro

Abstract: The purpose of this paper is to present a retinal vessel classification technique. First, in order to delimitate the area of interest, the optic disc is identified and modelled. The radius of the circle model is used as a parameter to extract the working area, which is outside of an inner circle concentric with the circle model and inside of an outer circle with a bigger radius. To localize the optic disc, a two steps technique was used: a) based on texture indicators and pixel intensity variance analysis in the green component of RGB image the optic disc area is roughly identified; b) disc edges are extracted and the resulted boundary is approximated by a Hough transform in the segmented area. Then from the thinned vessel image a vascular graph is extracted and filtered. The main branches of each connected sub-graph are identified starting from the graph edges near the optic disc. Various label configurations are propagated along each main branch edges and recursively along each secondary edge derived from the main one. The label propagation ends in case of conflicts at crossings. The no error label configuration or the one with the most classified edges is retained. The method has the advantages that the initial manual labelling of the starting vessels is no longer necessary and it is able to process high resolution images in which the line graph is too complex for other methods.

***Key words*:** hough transform, optic disc, landmark points, vessel graph, graph edge labelling.

1. INTRODUCTION

The retinal arteries and veins are differently affected by diseases as diabetic retinopathy, glaucoma, atherosclerosis or macular degeneration. The most observed indicator in such cases is the ratio between arteries and veins diameters (AVR). Usually the calibres of arteries decrease relatively to the calibres of veins, so AVR does. Another feature differently modified for arteries and veins is vessel tortuosity. To compute indicators as AVR or vessel tortuosity a classification of retinal vessels is necessary. The region of interest is nearby around the optic disc so the optic disc location and modelling are needed. Because the recognition and assessment of optic disc in retinal images are also tasks during the evaluation of the retina diseases as diabetic macular oedema or glaucoma, a vast literature on this subject was proposed. Some of the proposed methods, so called bottom-up techniques, locate directly the optic disc based on texture and intensity variance analysis. Another approach, namely top-down technique, identifies the main vessel branches and gets the optic disc area as the root of the vessels tree.

The bottom-up technique presented in [1] recognizes the optic disc and models it in two steps. First, three methods for an approximate identification of optic disc area are used: the maximum difference between the maximum and minimum grey levels in the working window, the maximum variance method and the frequency low pass filter method. The area of interest is located with a voting procedure: 1) if all three candidates are close to their centre then this one is proposed as the area centre; 2) if only two from three candidates are close to the centre the average point of these two is chosen; 3) if all candidates are far apart the candidate proposed by the second method is chosen. Secondly, in a 400×400 window centred on the estimated point previously chosen a morphological filter is employed as in [2] to erase the vessels in the window. Next, the optic disc edges are extracted with a Prewitt edge detector and the edge image is binarized using Otsu method [3]. The artefacts are eliminated by morphological erosion and finally a Hough transform is applied to get the final optic disc boundary. The second step of optic modelling is performed in both red

and green channels of the RGB original image and the circle with the best fitting score is finally chosen. Part of the optic disc area segmentation was implemented in our first algorithm to roughly locate the disc [4].

Once the optic disc was modelled, the working region would be the area located outside of a circle concentric with the disc model with a radius twice of the model radium and inside of a circle concentric with the first one with a radius eight times larger. The vessel labelling procedure includes the following main steps performed in the previously selected area: 1) vessel network segmentation; 2) network landmarks (branching, crossover, end points) extraction and analysis; 3) vessel graph generation and filtering; 4) graph edges classification. The main rules used by the final labelling process are: a) the 3D vascular structure is cycle free, so each binary tree included in the 2D vessel graph represents a vessel; b) in the vicinity of the optic disc area vessels at crossings are of different type (an artery never crosses an artery, the same for veins).

To perform the steps 2)-4) above for a full artery/vein (A/V) classification process, several methods have been proposed [6, 7, 8, 9]. The graph analysis proposed in [6] decides the type of each intersection point represented by a graph node. The nodes can be meeting point, or branch point, or cross point, depending on the orientation and the width of the incident vessel edges. The vessel width is computed based on initial vessel image analysis – from step 1 of the general labelling procedure. Then the vessels are classified using the rules a) and b) but for a large label domain. Finally, based on a combination of structural information and vessel intensity information, the domain of initial vessel labels is restricted to a binary domain (artery/vein) in two ways: by a supervised classification technique and by an unsupervised alternative. In [7], an initial labelling of the main vessels near the disc is manually performed. Then, in a grid of disjoint square cells of size 20×20 pixels, superimposed on the vessel image, each cell is analysed, starting from the optic disc area. The cell characteristics are computed as the number of connected components or the number of contacts of vessels with the cell edges. Based on previous cells and current cell characteristics the vessel type for the next cell is identified and propagated across the cell analysis. A percentage of 83.80% of correctly classified vessels is reported. The colour, the transverse intensity profile, and graph path properties of crossings and bifurcations of vessels were used as features in [8] to synthesize an energy function. To optimize the energy function by means of graph cuts, first a classification of the most significant six artery/vein pairs around optic disc is performed. Then in the area of interest the process is extended to the other pairs. An accuracy of 94.0% for the six widest vessels, respectively of 88.0% for all vessels, is reported. Another approach, presented in [9], proposes a heuristically AC-3 algorithm to differentiate in the graph the two vessel classes. The procedure propagates along the vascular tree the labels of some manually-classified starting vessel segments.

Our previous methods to label the retinal vessels were presented in [10] and [11]. We proposed a stratified strategy based on main vessels identification located in the optic disc vicinity. In [10] each main starting vessel is classified as vein or artery using an interactive classification technique. The established label is then propagated along the most significant descendant vessels. In [11] for each graph with at least two starting branches, various label configurations are used to classify the graph's secondary edges. The label propagation ends in case of conflicts at crossings. The no error label configuration or the one with the most classified edges is retained. The initial manual labeling for the starting vessels of each graph is no longer necessary. An improved (A/V) classification technique, tested on a new data set, is proposed in this paper.

The remainder of this paper is organized as follows. In Section 2 the optic disc area localization and modelling are presented. The preliminary retinal image processing techniques and network landmarks extraction and analysis [7] are summarized in Section 3. The proposed A/V classification algorithms are described in Section 4. The results are analysed in Section 5. The work is concluded in Section 6.

2. OPTIC DISC AREA LOCALIZATION

For a first attempt to locate the optic disc area we followed a similar methodology as the one proposed in [1]. From the three methods of the voting procedure presented in [1] we obtained good optic disc area localization with a modified Low-Pass Filter Method and the Frequency Low Pass Filter Method [4].

To cope with the image characteristics of public retinal image databases [12, 13], and specific databases provided by Grigore T. Popa University of Medicine and Pharmacy Iasi, mentioned in [4] and [5], a new method was proposed in [5]. The image was transformed in the frequency domain and the magnitude result of the FFT transform was filtered by a Gaussian low-pass filter [1]. The filtered result was transformed

back to the spatial domain. Using the histogram of the new image, a binarization threshold was computed. A 21×21 median filter was applied to eliminate isolated peaks. The result is the image $I(i,j)$. Each $I(i,j)$ pixel with a grey value greater than the threshold computed earlier is denoted "bright". On each "bright" pixel a square window of the same dimension as the one used by median filter was centred and the intensity pixel variance, denoted Var(i,j), was computed. Also, for every pixel $I(i,j)$, a texture measure was computed, using the Modified Maximum Difference Method [1]. A new image Diff(i,j) was generated. Each Diff(i,j) pixel is the difference between the maximum grey value and minimum grey value of the pixels inside a 21×21 window centred on the current $I(i,j)$ pixel:

$$\mathrm{Diff}(i,j) = I_W^{\max}(i,j) - I_W^{\min}(i,j).$$

An image, denoted $F(i,j)$, of normalized texture values, was created. Finally, the pixel $O(m,n)$ of image $I(i,j)$ with $F(m,n) > F(i,j)$ and $\mathrm{Var}(m,n) > 0.7\max(\mathrm{Var}(i,j))$, $0 \le I \le H-1$, $0 \le j \le W-1$, was declared as the centre of a window containing the optic disc.

Results of the new identification optic disc area procedure are depicted in Fig. 1. The original green channel is 1.a. The images $I(i,j)$ and $F(i,j)$ are illustrated by Fig. 1b and Fig. 1c. Black pixels in Fig. 1c are "dark" pixels of $I(i,j)$ not considered as possible optic disc centre candidates. The final result is depicted in Fig. 1d, where the cross indicates the centre of the working window in the selected channel.

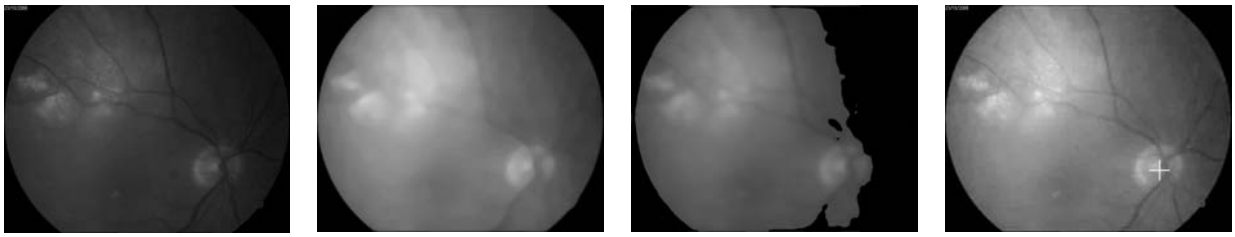

a. b. c. d.

Fig. 1 – Result of detecting an approximation of the optic centre position: a) green channel image; b) Gaussian filtering result; c) $F(i,j)$ image, where black pixels are "dark" pixels of $I(i,j)$; d) the cross indicates the working window centre [5].

In the located area, a morphological opening using a line as structuring element was performed for 12 orientations of the line, as in [2]. This operation eliminates blood vessels in the area and prepares it for optic disc border extraction. Which is accomplished by an iterative Canny filtering followed by binarization. When a number of edge pixels greater than a predefined threshold is obtained, the iterative operation stops. The optic disc model is computed using the Hough transform.

The optic disc modelling was performed errorless on images of DRIVE database [12], respectively "High-Resolution Fundus (HRF) Image Database" [13] used in retinal labelling process. The modelling results are illustrated in Fig. 2a, and Fig. 5b.

3. PRELIMINARY RETINAL IMAGE PROCESSING STEPS

A set of manually segmented images of the public DRIVE database [12] and a set of segmented images of HRF database [13] were the test input for our vessel labelling application. The working image synthesis is illustrated by Fig. 2a, b, c, using DRIVE [12] images (RGB original image and the manually segmented image):

1) The radius r of the circle model is used as a parameter to extract the working area in the thinned image of the vessel network;

2) From the DRIVE [12] vessel image (Fig. 2b) a centreline image, denoted TV, is generated by thinning;

3) A working image, noted RV, is built by deleting in TV image any vessel pixel outside the outer circle of radius 12r or inside the inner circle of radius 2r. The vessel graphs of RV images are filtered using a procedure described below. The filtering results are illustrated in Fig. 2c.

For landmark point set analysis and final A/V classification two other feature images are needed:

– A vessel width image, denoted WV;

– For each vessel pixel in TV image, the intensity variance in the green channel of the original colour image is computed, using a 14×14 window. The result is stored in a floating point array, noted VV.

By scanning the RV image, multiple point (vessel point with more than two vessel neighbours) structures are generated. The structure set is filtered to retain only the essential multiple points. The essential multiple point set of the RV image is ordered with respect to point distance to the optic disc centre. Besides the essential point coordinates each significant point structure includes also the coordinates of the nearest 2-neighbour vessel pixels considered as starting points for vessel tracking in the RV image. The tracking process generates a line structure including: line end points; essential points associated to end points; line length; tracked vessel pixel coordinates set; a binary attribute to mark the line as allocated (processed) during the graph structures generation process. Along tracking for each current pixel, there are picked from WV, VV and the green channel of RGB images the following parameters: vessel width; intensity variance and the grey level. At the tracking end, for short segments, the average of each parameter is computed. If the vessel length is greater than a threshold experimentally established, at each end just a fraction of the stored vessel points are used to compute the parameter average. The vessel slope is computed in the same manner, but this time using the coordinates of the whole set of stored vessel points or of a fraction of points at each vessel end. The line structure includes also a graph index, to indicate the graph membership. Then, each line structure is completed with pointers to the incident lines at its ends. For each incident line at crossings, the associated line index structure field is completed if the two lines have almost the same width, local orientation, intensity and variance means. Later, the line structures are filtered in order to: detect and delete short lines bounded by bifurcations that hide crossings and associate properly the remaining crossing segments; detect tangency situations and associate segments; eventually associate vessel segments at crossings with more than two vessels (four branches) [10, 11]. Also, the very thin branches connected to much more significant ones are eliminated in order to simplify the graph analysis [10, 11]. For images from the DRIVE database [12] the result of all line structures processing is depicted by Fig. 2c. For the HRF database [13], in cases of intersections of two vessels with much different widths, as depicted by Fig. 3a, a special configuration would be generated in the thinned vessel image, as depicted by Fig. 3c.

a. b. c.

Fig. 2 – a) Working area on an RGB image from the DRIVE database [12] (area outside of inner circle and inside of outer circle); b) manually segmented image; c) blood vessels graph.

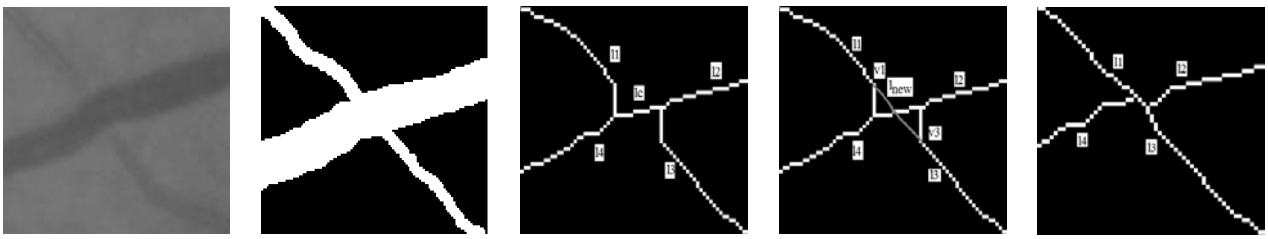

a. b. c. d. e.

Fig. 3 – a) Area intersection of two vessels with very different widths; b) the same area in the manually segmented vessel image; c) thinning result; d) line l_{new} induced by the inflexion points v_1 and v_3; e) final configuration.

In this case the following procedure is applied in order to associate the vessel segments at intersection.

1. For each secondary (thin) branch, l_1, respectively l_3, compute the inflexion point, v_1, respectively v_3, using the procedure proposed in [14]. If a significant inflexion point is not detected, the procedure is aborted.

2. In the working image: build the v_1v_3 line and erase the l_1 line points between v_1 point and its end connected to l_4 and l_c, respectively erase the l_3 line points between v_3 point and its end connected to l_2 and l_c.
3. Cancel the point structures of the essential points of l_1 and l_3 from their intersections with l_c. Add the point structure of the essential point generated by intersection of v_1v_3 line with l_c line.
4. Rebuild the line structure set using the new point structure set, generated at previous step. Update the widths and slopes at the working ends of new segments l_1 and l_3.

4. STRATIFIED RETINAL VESSEL LABELLING PROCEDURE

Graph structure sets are synthesized by tracking the pointers to incident lines at current line end, [10], [11]. First, the graph index of the line structure is set accordingly and the current line is marked as processed to avoid tracking cycles. After all line set was processed, for each line set with the same graph index, the main branches, starting from the inner circle of the working area, are identified. Each starting main branch is tracked in order to extract the rest of the main vessel and to fill the graph structure. The graph main branches detection procedure is described in Fig. 4.

```
Algorithm 1 Graph main branches detection
Input: Lines set
Output: Graphs set
1.  for each line set with the same index graph do
2.    if current line has one "1- neighbour" end located from
            inner circle at a distance less than
                a specific threshold
3.      if the "1- neighbour" end has at least two vessel
                neighbours in the original image of the
                thinned vessels
4.        if the starting segment has a significant length 5.
          index_starting_lines[nmb_starting_lines++] =
                current line index;
          else
6.          search each branch until branches of significant
                length are found;
7.          for each branch
8.            index_starting_lines[nmb_starting_lines++] =
                current branch index;
9.          end for
10.       end if
11.     end if
12.   end if
13. end for
14. reorder the index set, index_starting_lines[], and
        the others fields of the graph structure by starting
        segment  width (the largest width on first position ).
15. if nmb_starting_lines >=1 do
16.   for each starting_line  do
17.     current_line = starting_line;
18.     if current_line end is a "1-neigbour" end go to 7;
        end if
19.     if current line end has two incident lines
20.       branch_for_starting_lines[][]=current_line index;
21.       current_line = line with greatest width from two
              incident ones;
22.     end if
23.     if current line end has at least three incident lines
24.       branch_for_starting_lines[][]=current_line index;
25.       current_line = index of associated line at crossing;
26.       if the other lines at crossing are not associated
            fill the fields of non-associated lines at crossings;
28.     end if          // ifs on routine lines 26, 23
29.   end for
30. end if
```

Fig. 4 – Algorithm for graph main branches detection.

Step 3 of the **Algorithm 1** avoids considering as starting main branch segment an ending segment of a vessel located in the optic disc area. The main branches detection result is illustrated in Fig. 5b, for all connected sub-graphs.

The next step identifies for each connected sub-graph with at least two starting branches the set of associated crossing lines. If at least one four lines set, with line indices *i, j, k, n,* fulfilling the conditions *index_cross* of *Lines*[*i*] = *k*, *index_cross* of *Lines*[*k*] = *i*, *index_cross* of *Lines*[*j*] = *n*, *index_cross* of *Lines*[*n*] = *j*, is found out then a process to get the non-conflict label configuration or the one with the most correctly labels is started. In what follows, the labels denoted "0" are allocated to the veins and the "1" labels are given to the arteries. Starting from the label configuration $\{0_1, 0_2, ..., 0_m\}$ allocated to the start segment set of the main branches, the labelling process continues with the rest of possible configurations until the right starting label set is found. Meaning that for all *i, j, k, n* associated crossing lines the labelling fulfil the rule b) of the classification process: *label* of *Lines*[*i*] = *label* of *Lines*[*k*], *label* of *Lines*[*j*] = *label* of *Lines*[*n*] and *label* of *Lines*[*i*] ≠ *label* of *Lines*[*j*].

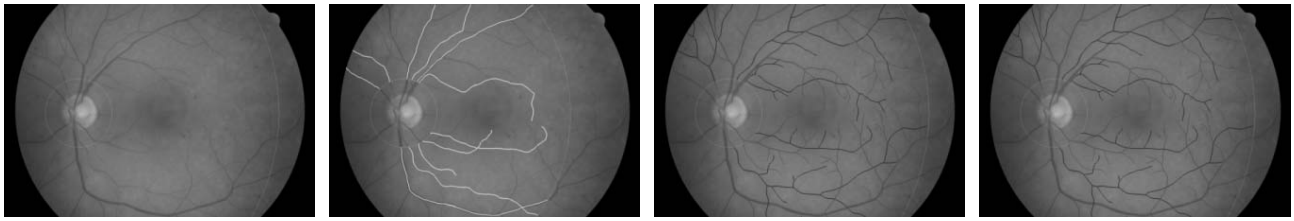

a. b. c. d.

Fig. 5 – a) Original high resolution RGB image; b) main branches of all connected sub-graphs; c) alg. 2 result; d) final result.

Due to the reordering of step 14 in the above algorithm, the first position of initial label set would be always allocated to a vein because in the optic disc vicinity veins have larger diameters than arteries. So the labelling process would be finished in the worst case when the first configuration of type $\{1_1, x_2, \ldots x_m\}$ is reached. The procedure to get the right starting label configuration is shown in Fig. 6.

Algorithm 2 Graph structures labelling validation
Input: Current graph, label configuration for main branches
Output: 0 = error at crossings or 1 = no errors; number of labelled vessels.

```
1.  for each main branch (starting_line) do
2.    for each line in current main branch do
3.      initialize a line index stack; stack_level = -1;
4.      error_flag = 0;
5.      current_line = current line from main branch;
6.      label = current_line label //(artery = 0, vein = 1)
7.      do  //recursive labelling
8.        if current_line it is not labelled
9.          current_line label = label;
10.       else if current_line is not a main branch line
11.         return 0;
12.       end if //ifs on routine lines 10, 8
13.       if current_line end is a "1-neigbour"
14.         if stack_level < 0 go to 2; end if
15.         current_line = current line from index_stack.
16.         stack_level--;
17.       end if     // if on line 13
18.       if current line end has two incident lines
19.         if both incident lines have widths less than current
                line
20.           current_line = incident line with greatest width;
21.           stack_level++; push the second incident line
                index;
22.           continue; //resume do loop
              else
23.           if stack_level < 0 go to 2; end if
24.           current_line = current line from index_stack;
25.           stack_level--; continue;
26.       end if   //ifs on routine lines 19, 18
27.       if current line end has three incident lines
28.         if current line is associated
29.           current_line = index of associated line at
                crossing;
30.         if the other two lines at crossing are associated
              and are labelled with the same value as
              current label
31.           return 0;
32.         if the other two lines at crossing are not
              associated fill the fields of non-associated
              lines at crossings;
33.         continue;
34.         else if the other two lines at crossing are
              associated
35.         find out the index of the other non-associated
              line;
36.         if the width of the line is of the same range as
              current one
37.           current_line = current other line; continue;
38.         if stack_level < 0 go to 2; end if
39.           current_line = current line from index_stack;
40.           stack_level--; continue;
41.     end if  // ifs on routine lines 36, 34, 32, 30, 28, 27.
42.   end do
43. end for….// for on routine lines 1, 2.
44.     return 1;
```

Fig. 6 – Algorithm for graph structures labelling validation.

Besides the optimal starting label configuration, **algorithm 2** leads to the classification of the main vessel of the entire blood network. Also, along the classification process a list of ambiguous labelling cases is generated. An **algorithm 2** result is depicted in Fig. 5c. In the last phase of the labelling process, when more information is obtained, the ambiguous cases would be reconsidered using **algorithm 3**.

Algorithm 3 (Fig. 7) includes the labelling procedures for all unsolved cases gathered along the first two steps of the classification process:

- Not labelled pairs of vessels derived from a labelled main vessel. The non-labelled pairs that do not fulfil any association condition are considered secondary branches of the main labelled branch;
- Not labelled vessel from an intersection with two other associated and labelled vessels and a third vessel with a different label than the associated pair;

– Not labelled vessels from four or five incident vessels groups where only the main vessel is classified;
– Not labelled vessels from at least five vessel intersections with two tangent vessels.

Figure 5d shows a result of **Algorithm** 3. The final version of the entire A/V classification process is presented below. The final A/V classification results are illustrated for high resolution images in Fig. 9.

Algorithm 3 Not-marked branch labelling at crossings
Input: Labelled graph produced by Algorithm 2
Output: Graph with new labelled vessels
1. **for** each pair of not associated line in the list **do**
2. **if** line pair is labelled continue; **end if**
3. **if** lines in the same width and orientation ranges continue; **end if**
4. **if** the other line pair at crossing is not labelled continue; **end if**
5. label = label of the other line pair //(artery 0, vein 1)
6. **for each** line in the pair **do**
7. initialize a line index stack; stack_level = -1;
8. error_flag = 0;
9. *current_line* = current pair line;
10. **do** the recursive labelling of Algorithm 2 (lines 7-43) **end do**
11. **end for**
12. **end for**

Fig. 7 – Algorithm for not-marked branch labelling.

Main Algorithm
Input: *Graphs* set
Output: *Graphs* set with labelled vessels
1. **for each** *Graph* structure **do**
2. Graph main branches detection - Algorithm 1
3. **for each** label configuration of the graph main branches **do**
4. result = Graph structures labelling validation – Alg. 2;
5. save label configuration with the most labelled branches;
6. **if** result > 0
7. Not-marked branch labelling at crossings - Alg. 3;
8. go to 1;
9. **end if**
10. **end for**
11. use the label configuration saved in step 5 to label the graph;
12. Not-marked branch labelling at crossings – Algorithm 3;
13. **end for**

Fig. 8 – The main algorithm.

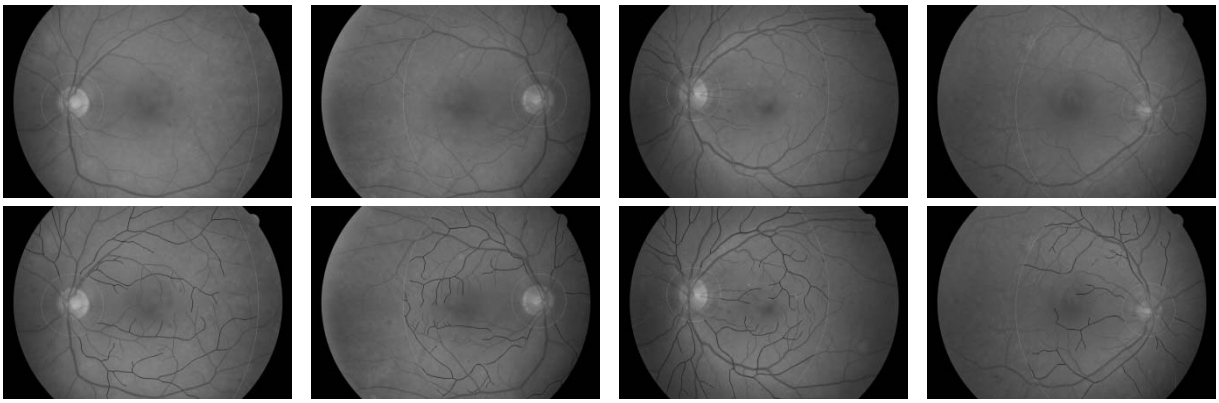

Fig. 9 – Original RGB high resolution images, upper row; Classification result, bottom row.

5. RESULTS

The proposed method was tested on a set of 30 images of the DRIVE database [12] and also on a set of 20 high resolution (3504×2336) images from the HRF database [13]. To evaluate the results, the following indicator was used: $R = \sum(w_i l_{cls_i}) \Big/ \sum(w_i l_i^{init})$, where l_{cls_i} is the length of the i^{th} vessel correctly classified; l_i^{init} is the length of the i^{th} vessel from working area. The weight w_i is defined as: $w_i = 0.1 + 0.9 \times (width_i - width_{min}) / (width_{max} - width_{min})$, where $width_i$ is the i^{th} vessel width, $width_{min}$ is the minimum width for all the vessel network and $width_{max}$ is the maximum width. For the DRIVE [12] images, the average of the correct classification rate was 95.1%. For the high resolution set, an average of 92.2% correct classification rate was obtained. Due the fact the recognition rate is computed differently by almost every paper it is difficult to compare exactly the overall results. However, considering also that working area is considerable larger than the one used by other authors, we appreciate that our results are ones of the best in field.

6. CONCLUSIONS

The proposed method was validated using two different databases. The first test was performed by using a set of 30 images of the DRIVE database, which was used also in our previous work [11]. Compared to the other methods presented in the literature, the proposed A/V labelling method has two main advantages: (a) the analysed area of interest around the optic disc is much larger than the one considered in other similar works and (b) initial manual labelling for the starting vessels of each graph it is no longer necessary. The proposed improvements of the line set analysis, presented in this paper, lead to a slight increase of the recognition rate: 95.1% versus 95%. The second test was performed by using high resolution retinal images. Due the fact that the line graph is much more complicated, the line set filtering has been completed to cope with new possible configurations. For a set of 20 high resolution images a recognition rate of 92.2% was obtained. The main gain of the propose method consists in the algorithm improvement to cope with high resolution images without the need to adjust the parameters of the algorithm.

ACKNOWLEDGMENTS

This research was supported by the Romanian Academy as part of the project *Signals analysis and recognition, Information fusion,* research theme *Methods of artificial intelligence in biomedical images analysis.*

Authors' contributions. The authors equally contributed.

REFERENCES

1. A. AQUINO, M.E. GEGUNDEZ-ARIAS, D. MARIN, *Detecting the optic disc boundary in digital fundus images using morphological, edge detection, and feature extraction techniques*, IEEE Trans. Medical Imaging, **29**, *11*, pp. 1860-1869, 2010.
2. C. HENEGHAN, J. FLYNN, M. O'KEEFE, M. CAHILL, *Characterization of changes in blood vessel width and tortuosity in retinopathy of prematurity using image analysis*, Med. Image Anal., **6**, pp. 407–429, 2002.
3. N. OTSU, *A threshold selection method from gray-level histograms*, IEEE Trans. Systems, Man, and Cybernetics, **9**, *1*, pp. 62-66, 1979.
4. F. ROTARU, S. BEJINARIU, C.D. NIȚĂ, M. COSTIN, *Optic disc localization in retinal images*, in: Balas V., Fodor J., Várkonyi-Kóczy A., Dombi J., Jain L. (eds.) *Soft Computing Applications. Advances in Intelligent Systems and Computing*, **195**, Springer, Berlin, Heidelberg, 2013, pp. 453-463.
5. F. ROTARU, S. BEJINARIU, C.D. NIȚĂ, R. LUCA, C. LAZĂR, *New optic disc localization approach in retinal images*, 2013 E-Health and Bioengineering Conference (EHB), Iași, pp. 1-4, 2013.
6. B. DASHTBOZORG, *Advanced Image Analysis for the Assessment of Retinal Vascular Changes*, Ph.D Thesis, University of Porto, 2015.
7. E. M. FELIPE-RIVERON, F. M. V. CASTALDI, E. S. GÓMEZ, M. A. L. VASCONCELLOS, C. ALBORTANTE MORATO, *A Semi-supervised Puzzle-Based Method for Separating the Venous and Arterial Vascular Networks in Retinal Images*, Springer, Pattern Recognition, Proc. 6th Mexican Conf. (MCPR 2014), Cancun, Mexico, 2014, pp. 251-260.
8. B. M. H. ROMENY et al., *Brain-inspired algorithms for retinal image analysis*, Machine Vision and Applications, **27**, pp. 1117–1135, 2016.
9. K. ROTHAUS, X. JIANG, P. RHIEM, *Separation of the retinal vascular graph in arteries and veins based upon structural knowledge*, Image and Vision Computing, **27**, pp. 864–875, 2009.
10. F. ROTARU, S.I. BEJINARIU, C. D. NITA, R. LUCA, M. LUCA, A. CIOBANU, *Retinal Vessel Classification Technique*, in: Balas V., Jain L., Balas M. (eds.) Soft Computing Applications (SOFA 2016): *Advances in Intelligent Systems and Computing*, **634**, Springer, Cham, 2017, pp. 498-514.
11. F. ROTARU, S.I. BEJINARIU, C. D. NIȚĂ, R. LUCA, A. CIOBANU, M. LUCA, *Retinal vessel labeling technique*, 2017 E-Health and Bioengineering Conference (EHB), Sinaia, 2017, pp. 109-112.
12. J.J. STAAL, M.D. ABRAMOFF, M. NIEMEIJER, M.A. VIERGEVER, B. VAN GINNEKEN, *Ridge based vessel segmentation in color images of the retina*, IEEE Transactions on Medical Imaging, **23**, pp. 501-509, 2004.
13. A. BUDAI, R. BOCK, A. MAIER, J. HORNEGGER, G. MICHELSON, *Robust Vessel Segmentation in Fundus Images*. International Journal of Biomedical Imaging, 2013, pp. 1-11.
14. F. ROTARU, S. BEJINARIU, M. BULEA, C. NIȚĂ, R. LUCA, *Adaptive recognition method for 2D polygonal objects*, ISSCS 2011 – International Symposium on Signals, Circuits and Systems (ISSCS), Iași, pp. 1-4, 2011.

Received June 6, 2018